Michigan Technological University

Digital Commons @ Michigan Tech

Dissertations, Master's Theses and Master's Reports

2018

Novel Faraday Rotation Effects Observed In Ultra-Thin Iron Garnet Films

Brandon Blasiola
Michigan Technological University, bdblasio@mtu.edu

Recommended Citation

NOVEL FARADAY ROTATION EFFECTS OBSERVED IN ULTRA-THIN IRON
GARNET FILMS

By

Brandon Dominic Blasiola

A THESIS

Submitted in partial fulfillment of the requirements for the degree of

MASTER OF SCIENCE

In Applied Physics

MICHIGAN TECHNOLOGICAL UNIVERSITY

2018

This thesis has been approved in partial fulfillment of the requirements for the Degree of MASTER OF SCIENCE in Applied Physics.

Department of Physics

Thesis Advisor: *Miguel Levy*

Committee Member: *Jae Yong Suh*

Committee Member: *Durdu Guney*

Department Chair: *Ravindra Pandey*

Table of Contents

Acknowledgements

I would like to thank Miguel Levy for his advisement and overseeing of my research, allowing me the freedom to work while ensuring that I did not waste any time or resources. I also would like to thank Chito Kendrick for his assistance and instruction on the various equipment and labs located in the Microfabrication Facility. I thank Dolendra Karki for introducing me to the Levy group and showing me the ropes in my first year. I also would like to thank Michigan Technological University for its commitment to graduate students and its various facilities and resources, without which much of the work presented herein would not have been possible.

Abstract

Recent work performed by A. Chakravarty and M. Levy showed experimentally a dramatic increase in the specific Faraday Rotation (FR) of the iron garnet $Bi_{0.8}Lu_{0.2}Gd_2Fe_5O_{12}$. A theoretical model, based purely on classical electrodynamics, attempting to explain this behavior was developed by colleagues in Russia that not only confirmed the asymptotic increase in the specific FR at sub-50nm film thicknesses but also suggested that the specific FR should exhibit significant fluctuations at sub-500 nm film thicknesses. The original data points were widespread with steps of 50 nm or more between data points that skipped over the theoretical oscillations. Presented herein are the results of performing high-resolution data point steps of 5-15 nm with the intent of catching the oscillations. We have obtained data that confirms the presence of significant oscillations at thicknesses below 100 nm and have reconfirmed the behavior previously shown at ultrathin thicknesses. While the proposed model confirms some of the basic features of the original experimental data and makes additional predictions, now confirmed through the work reported in this thesis, further analysis is still needed to fully explain the observed experimental results. We have also included some possible explanations for this phenomenon.

1 Introduction

1.1 Background

The field of photonics focuses on photon transmission and light-matter interaction and the phenomena that drive these processes[1]. Many advancements and discoveries have been made over years of research in this field; among these discoveries is the phenomenon known as Faraday rotation. Faraday rotation is a magneto-optical effect that is a property of some special materials that changes the polarization angle of polarized light that transmits through the material. When these materials – in our case, iron garnets – are in the presence of a magnetic field, the optical properties of the material are changed. The material begins to exhibit circular birefringence meaning that the optical index for right-hand circularly polarized (RHCP) light is different than the optical index for left-hand circularly polarized (LHCP) light. When a linearly-polarized beam of light propagates through a regular medium such as air, the RHCP and LHCP components propagate at the same speed. However, when linearly polarized light is transmitted through one of these circularly birefringent materials, the RHCP and LHCP components that form the linear polarization propagate at different speeds which causes a phase change to occur between the two components. When the light exits the material, the RHCP and LHCP once again propagate at the same speed and due to the change in phase between the two components, the overall linear polarization angle is different. The difference between the initial and final polarization angles in what we define as the Faraday rotation. Because the amount of Faraday rotation is dependent on the amount of material the light transmits through, it is usually more useful to refer to the *specific* Faraday rotation. That is, we normalize the Faraday rotation to the thickness of the material to make it easier to observe if there are any deviations from the bulk value of the Faraday rotation.

Because the Faraday rotation is dependent on the strength of the magnetic field in which the sample is placed, we take our measurements a what is called the saturation field strength of the material. At saturation, the material gives no further response to the magnetic field from magnetic domain misalignment, and the Faraday rotation effect is, in effect, maximized. The saturation value remains nearly the same for any thickness of the material which allows for accurate, repeatable measurements.

1.1.1 Faraday Rotation

Faraday Rotation, also known as the Faraday effect, as stated previously, is a consequence of circular birefringence. The natural progression of thought leads one to wonder what causes circular birefringence. The driving phenomenon for this birefringence is based in how the permittivity tensor of a magneto-optic material reacts to a magnetic field. The permittivity tensor, when under the influence of a magnetic field, has the general form:

$$\epsilon = \begin{bmatrix} \epsilon'_{xx} & \epsilon'_{xy} + ig_x & \epsilon'_{xz} - ig_y \\ \epsilon'_{xy} - ig_z & \epsilon'_{yy} & \epsilon'_{yz} + ig_x \\ \epsilon'_{xz} + ig_y & \epsilon'_{yz} - ig_x & \epsilon'_{zz} \end{bmatrix}$$

With symmetrical matrix ϵ' and gyration vector, g. The gyration vector is related to the magnetic field by the relationship $g = \epsilon_0 \chi^{(m)} H$. In this relationship, $\chi^{(m)}$ is known as the magneto-optical susceptibility. The susceptibility quantifies the polarization potential of a material based on the applied field. If the gyration vector is an eigenvector of ϵ' and we allow light to propagate in the direction of the gyration vector, the permittivity tensor can be simplified to:

$$\epsilon = \begin{bmatrix} \epsilon_1 & \epsilon'_{xy} + ig_x & \epsilon'_{xz} - ig_y \\ \epsilon'_{xy} - ig_z & \epsilon_1 & \epsilon'_{yz} + ig_x \\ \epsilon'_{xz} + ig_y & \epsilon'_{yz} - ig_x & \epsilon_2 \end{bmatrix}$$

Furthermore, if we make it so **g** lies in the z-direction, we obtain the simplest form of the permittivity tensor:

$$\epsilon = \begin{bmatrix} \epsilon_1 & +ig_x & 0 \\ -ig_z & \epsilon_1 & 0 \\ 0 & 0 & \epsilon_2 \end{bmatrix}$$

The explanation for the Faraday effect resides with the solutions of this matrix. If light propagates through this material, it does so with a phase velocity of $\frac{1}{\sqrt{\mu(\epsilon_1 \pm g_z)}}$. The linearly polarized light that is incident on the material exists as a superposition of RHCP and LHCP light. The RHCP light has phase velocity $\frac{1}{\sqrt{\mu(\epsilon_1 + g_z)}}$ and the LHCP has phase velocity $\frac{1}{\sqrt{\mu(\epsilon_1 - g_z)}}$. The difference between these two phase velocities causes a Faraday rotation to occur.

1.1.2 Discussion of Iron Garnets

It is natural to consider what makes iron garnets capable of supporting Faraday rotation. The composition of these iron garnets follows the form $X_3Fe_5O_{12}$, where X is an element or number of elements that compose a total of 3 parts. A common and simply composed iron garnet Yttrium Iron Garnet has the composition $Y_3Fe_5O_{12}$, whereas the samples used in the presented research was Bismuth-Lutetium-Gadolinium Iron Garnet with the composition $Bi_{0.2}Lu_{0.8}Gd_2Fe_5O_{12}$. While this 3-5-12 formula is simple, it does not accurately represent the structure of the iron garnets. The magneto-optic behaviors of these garnets are the result of the iron ions that reside in specific locations in the lattice structure, which consists of two octahedral regions, three tetrahedral regions, and an irregular cube formed by oxygen ions[5]. The substitution of bismuth, lutetium, or some other post

transition metal or lanthanide changes the gyrotropy of the substance leading to a change in the magnetic saturation field strength.

1.1.3 Classical Model/Internal-Reflections model

The light that is subjected to the Faraday Effect via transmission through a magneto-optic film in the presence of a magnetic field is also subjected to three other behaviors: absorption, transmission, and reflection. As it is with all light that interacts with different media, there exists no less than one interface between media. In the research presented herein, there are two interfaces: the air-to-film interface where the light enters the film and the film-to-air interface where the light exits the film. At each interface, some amount of the light is either reflected away from or transmitted across the interface. For normal incidence, the amount of light that is reflected or transmitted is given by the following relationships knows as reflection (R) and transmission (T) coefficients:

$$R = \left|\frac{n_1 - n_2}{n_1 + n_2}\right|^2$$

$$T = 1 - R$$

Light that is transmitted across the interface continues onward undergoing no more Faraday Rotation. However, light that is internally reflected has its polarization angle mirrored from reflecting and continues in the reverse direction undergoing further Faraday rotation, in the same direction. Upon reaching the initial interface, some of the light is transmitted across and lost while the rest is once again reflected internally, having its polarization angle mirrored again and undergoing more Faraday Rotation. This process continues until all of the energy of the light is either absorbed or transmitted. The nature of these reflections means that every odd-numbered beam contributes to the total Faraday Rotation, as seen in Figure 1 below.

An important behavior to note is how RHCP and LHCP light respond to the direction of the Faraday Effect. RHCP light propagating in the positive z-direction and LHCP propagating in the negative z-direction experience a Faraday Rotation in the same direction. That is, if one were to observe the polarization of the light by looking along the z-axis in the negative direction, one would observe a clockwise rotation of the polarization for both the RHCP and LHCP light. This direction of rotation given here is merely for demonstrative purpose.
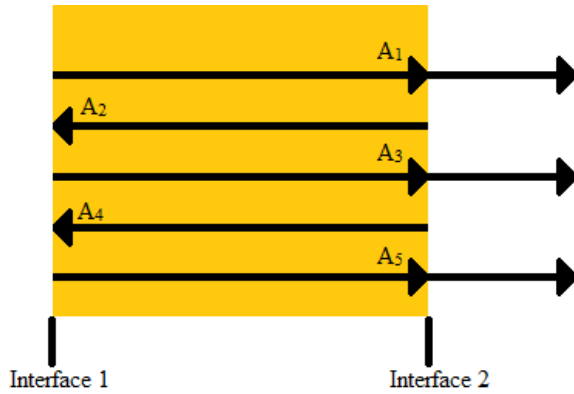
Figure 1, *Odd-numbered beam contribution*

1.2 Previous Work and Motivation

Data collected by Ashim Chakravarty several years ago showed that as the thickness of BiLuGdIG is reduced below 100nm, the value of the specific Faraday Rotation begins to increase dramatically from an approximately constant "bulk" value. It was found that this enhancement was partially due to geometric changes in the structure leading to a different behavior of the diamagnetic transitions of which Faraday Rotation is a consequence[2]. This result was subsequently confirmed with a theoretical model put together by colleagues of
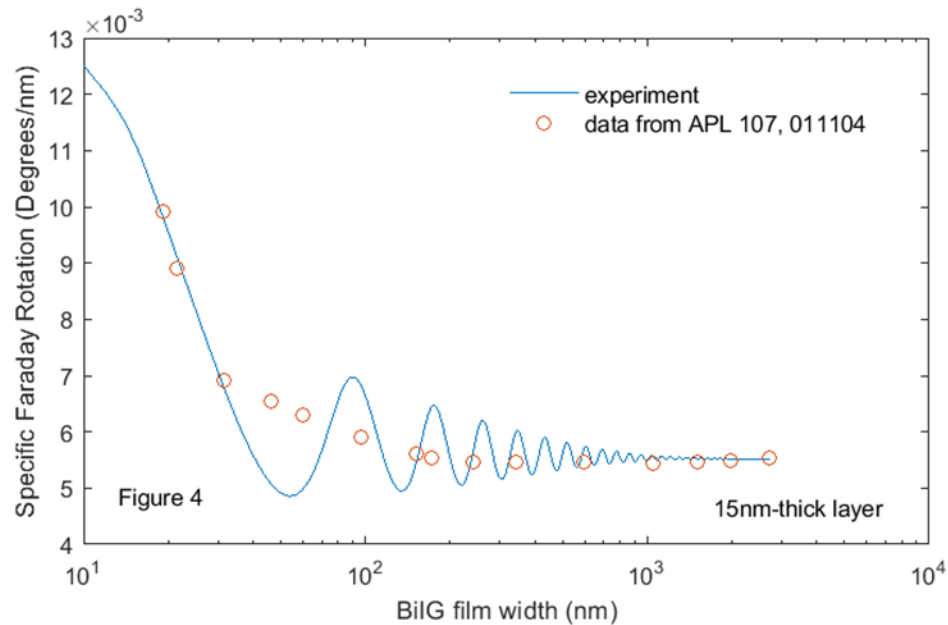

Fig. 2. *A. Chakravarty's data (red) and Model from O. Borovkova and V. Belotelov*

ours at the Russian Quantum Center in Moscow, Russia (Figure 1). Interestingly, though, the model also showed that the value of the specific Faraday rotation should not only increase dramatically as the thickness approaches zero in the nanometer range, but also

4

oscillate with increasing amplitude prior to the asymptotic increase. The original set of data obtained by A. Chakravarty was low-resolution and missed the peaks and valleys of these predicted oscillations. The goal of the research presented here was to take high-resolution data to "fill in the gaps" between the other data points and to find out whether or not the oscillations are a genuine phenomenon or an artifact of the model.

2 Methods

The experimental work for this project consisted of three core components: the measurement of the thickness of the film using ellipsometry, the measuring of the Faraday Rotation, and the removal of material via wet-etching. The steps of the data collection process are presented in this order because this is the same order in which the research was performed: The thickness of the film was verified by ellipsometry, a baseline bulk specific Faraday Rotation value was obtained, and the film thickness was reduced in order to repeat the process. The sample we are using is sourced from Integrated Photonics, Inc. and was grown using liquid-phase epitaxy (LPE). Samples grown via LPE are mono-crystalline and thus, of higher quality and better overall uniformity than samples that are sputter or pulsed-laser- deposited on a lattice matching substrate. We prefer to use these samples because we do not want there to be any anomalous results from inconsistencies in the sample's composition. The piece of LPE-grown BiLuGdIG that was used in the research presented here was cut from a larger sample and has dimensions 3 x 5 mm.
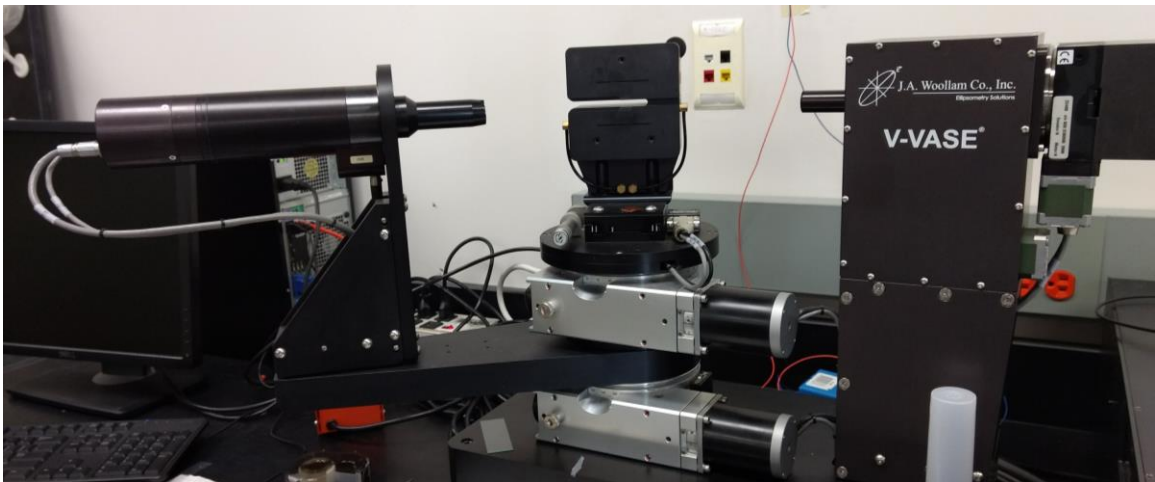
2.1 Thickness Measurement

Fig. 3. *The Ellipsometer*

The thickness measurement of the original sample was the first step in this research. We wanted to verify the specified value for the thickness given to us by the manufacturer of the sample. Knowing the starting point is essential for a couple of reasons: first, if we do not know where we are starting, we have no idea how much film to etch away, and if we aren't careful, we could accidentally remove the film entirely and be left with nothing but the substrate. A second reason to measure the thickness first is explained by our desire to have a baseline measurement of the specific Faraday rotation. The core topic of this project was to investigate potential variations from bulk measurements. If we used the specified thickness and the specified thickness was incorrect, then our baseline for the specific FR would be useless.

The thickness measurements were performed using the J.A. Wollam ellipsometer. A simple diagram of the apparatus is shown below.
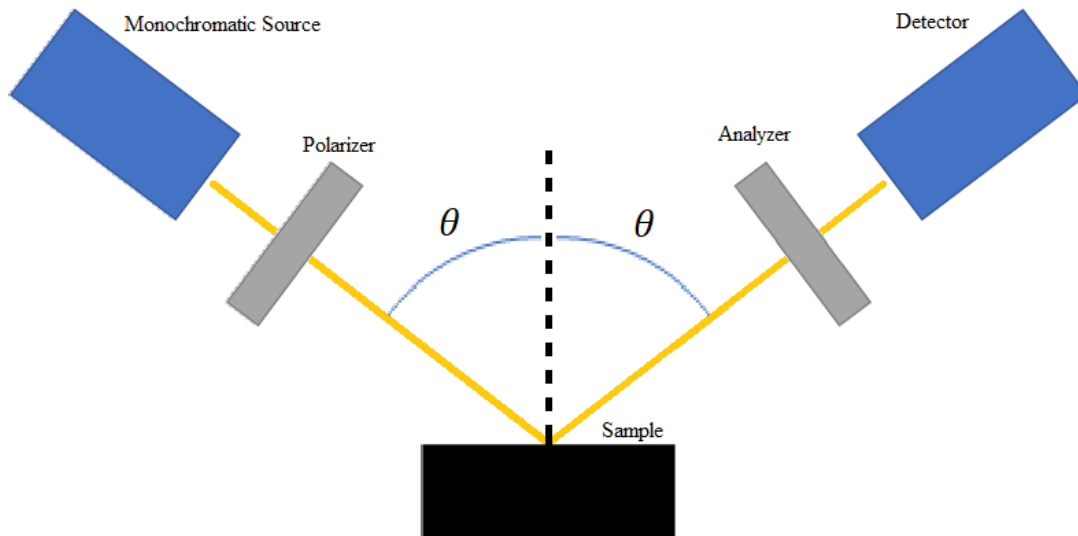

Figure 4, *Diagram of Ellipsometer*

The structure of the ellipsometer consists of four major components: the tunable monochromatic light source, the sample holder, the beam detector, and the computer and software that run the device. The basic operation of the apparatus involves light interacting with a sample which will modify the polarization and cause energy loss due to energy absorption. Because these changes are different for different wavelengths, we use the tunable monochromater to obtain data for wavelengths between 6000 and 16000 Angstrom. The ellipsometer also measures the change in energy which is dependent on the angle of incidence of the light, so we collect several data sets at different angles. The angles used throughout this research were 65, 70, and 75 degrees. We know that in addition to being wavelength and angle of incidence dependent, these changes are also dependent on the thickness of the film.

The ellipsometer collects a value for the polarization, or phase, and a value for the change in energy as a ratio of amplitudes. These sets of data are plotted as functions of wavelength resulting in three curves. There exists a function that uses the amplitude ratio, phase, and thickness that will reproduce these curves given the correct parameters. Several of these parameters are the index of refraction of the film, an estimation of film thickness, and some information about the substrate if one is present. The software then attempts to solve for the thickness by adjusting the parametric values to minimize the mean-square error. This process gives us a value for the thickness that has nanometer- to sub-nanometer accuracy.

2.2 Faraday rotation Measurement

The apparatus used to measure the Faraday rotation is one that was designed and built by Joe Dillon at Bell Labs in the 1960s. The apparatus was gifted to Miguel Levy in 2005 and various adjustments and improvements have been implemented since. Among these improvements are the addition of a lock-in amplifier and computer-integration using LabVIEW as a user interface and data recording software. The design of this apparatus is a bit complicated, but each part is essential to its operation. For reference to beam and signal path, see the following figure.
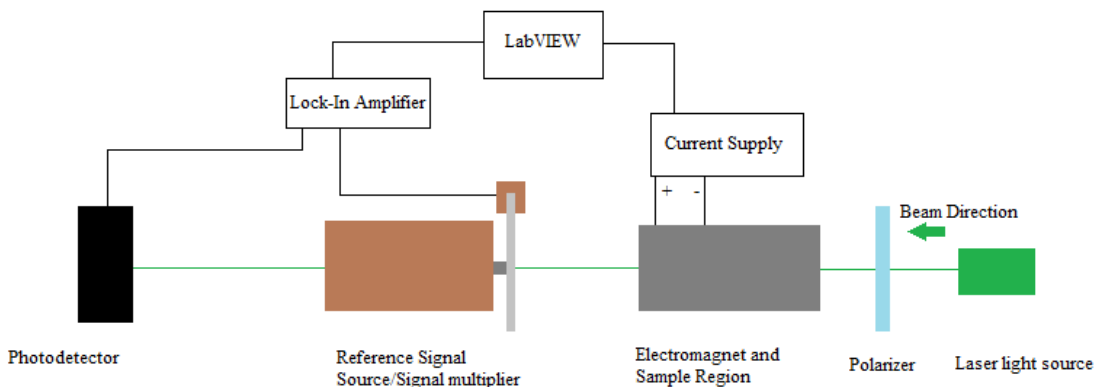

Figure 5, *Faraday Rotation Apparatus Diagram*

2.2.1 Laser and Polarization

In order to measure the Faraday Rotation, we must have polarized light. We transmit laser light through a polarizer to ensure an arbitrary polarization. The actual polarization does not matter for this measurement because we are not measuring an absolute Faraday Rotation but a relative one. This reduces the complexity of the experiment by removing the need to know the absolute angle of polarization. Additionally, while we used laser light with wavelength 532nm, we are not restricted to this specific wavelength; we use 532nm because it has a strong response for this specific material.

2.2.2 Electromagnet and Sample Region

Once the light is polarized, we must expose the sample to a magnetic field. In our case, we place the sample in a Teflon holder that is placed near the center of the field produced by a two-core electromagnet. The strength of this field is determined by the current running through the magnet. In order to determine what the maximum field strength of the magnet should be, we look at the saturation point of the sample. The saturation point is when the Faraday Effect no longer responds to a stronger magnetic field. For this research, the saturation field strength has been measured by D. Karki to be near 0.5298 Tesla at a current

of 7.0 A. The current is adjusted in increment s of 0.1 to 0.01 A depending on the time available to collect data or the desired resolution of data. We also have implemented n the program a brief relaxation period for each current level in order to allow the sample to stabilize.

2.2.3 Reference Signal

The third portion of the apparatus is a water-cooled motor. The motor has tubular main shaft and a polarizer allowing the light to pass through and an attached disk that has 32 slots cut out of it. As the shaft of the motor rotates, these slots pass through a photogate and multiply the frequency of a reference signal 32 times—an essential process that provides for functionality and resolution. The Faraday rotation is measured using a lock-in amplifier by comparing the reference signal to the final output signal of the system. The phase difference between these two signals is usually very small and we multiply the signal to get an improved response from the lock-in. To get an idea of the order of magnitude, the specific Faraday rotation for our sample is 4.5 degrees/μm. With a sample thicknesses as thin as tens of nanometers, the total rotation can be as little as $0.01 - 0.1$ degrees. The lock-in amplifier can rectify the phase difference more easily and more accurately when we multiply the signal.

2.2.4 LabVIEW Implementation and Data Collection

The final component of the apparatus itself is the photodetector, the output of which is sent to the lock-in amplifier. This measured signal is what the lock-in amplifier compares to the reference. These data of course mean nothing if they are not collected and recorded. The data recording process of our apparatus is computer-controlled using a LabVIEW program written and edited by A. Chakravarty and D. Karki. The program directly controls the current to the electromagnet and records the information received from the lock-in. These two data sets provide x- and y-axis data, respectively. The collection of the data forms a hysteresis loop from which we obtain the Faraday rotation. The specific FR is henceforth obtained.

2.3 Material Etching

The natural progress of making measurements requires that we reduce the thickness of the material. In general, there are a few different ways we can do this: mechanical etching or chemical etching. Mechanical etching is a process by which the material is physically removed by a polishing disk or lapping film. While this process is effective and usually simple, it can be too aggressive for some samples. The danger of damaging the sample is enough to prevent us from using this method. Another consequence of mechanical etching is the roughness of the surface. With physical, mechanical etching, small particles scrape over the surface. The gaps between these particles can leave tiny grooves causing the surface of the material to be uneven and nonuniform.

A second category of etching is chemical etching. Chemical etching comes in two forms: dry and wet. Dry chemical etching includes processing such as plasma etching, a process by which the surface-layer atoms react with a plasma and are subsequently removed. This form of etching is usually used for semiconducting materials like silicon in the production of integrated circuits. Plasma etching also has limitations on the presence of metals in the chamber. While our sample is not a pure metal, the presence of iron could prove to be problematic.

With two of three methods decidedly turned down due to undesirable outcomes, we are left with wet etching. Wet etching occurs when a sample is immersed in a liquid substance that can remove material. The liquid can evenly remove material from the sample without causing any damage from physical pieces colliding with it. For our processes, we use 85% phosphoric acid. Phosphoric acid has long been used for etching iron garnet and is reliable and consistent. The etch rate of the acid at room temperature is incredible slow, so we increase the etch rate by heating the acid to a temperature of at least 100 degrees Celsius. We are able to obtain etch rates in the range of 35-60 nm/minute. Wet etching in phosphoric acid has the additional advantage that it does not introduce lattice damage in the iron garnet materials.

For the actual process of wet-etching, a sample is placed film-side down in a 100 mL beaker filled with phosphoric acid. The beaker is stationed on an electric heating plate that is equipped with a magnetic stirrer. The acid is stirred to ensure that the acid has a constant, evenly distributed temperature. Uniform distribution of heating is important because the etch rate is slightly temperature-dependent. By varying the temperature and stirring speed, we can modify the etch rate for the desired outcome to rates as high as 100 nm/min.

2.4 Data

The data that is collected via this apparatus requires some rather simple analysis to "iron out" some kinks that are artifacts of the data collection apparatus. One of these artifacts is over-rotation. The lock-in amplifier measures phase differences up to 180 degrees. Due to the 32-times multiplier present in the system, some of the thicker films can produce a total phase difference that is greater than +/- 180 degrees. This causes rollover in the phase measurement that must be manually adjusted. A second artifact that requires manual removal is the calibration of the Faraday rotation about the zero-point. Different factors in the lab such as noise caused by light or initial polarization anomalies can cause the Faraday rotation to appear to be present at zero-field. When we calibrate, we see how the Faraday rotation behaves in the positive and negative field strengths. The final artifact that we must deal with is determining the overall value of the Faraday rotation. We find the arithmetic mean of the "positive" and "negative" saturation values of the hysteresis loop. We do this because the film doesn't know which direction the light is transmitting through it.

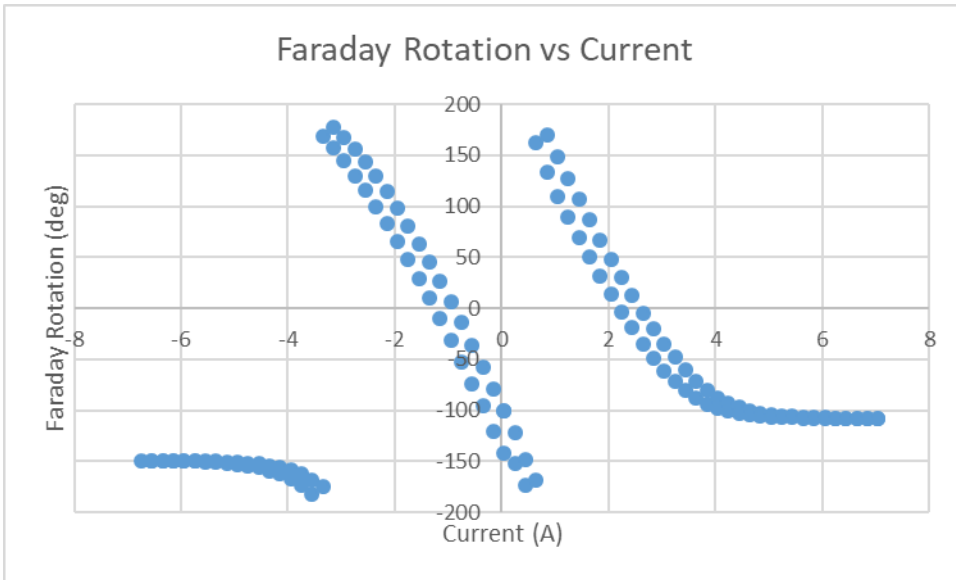Presented below is an example of raw data for the film at thickness 2.1 μm.

Fig. 6. *Raw Data for 2.1 μm*

The first artifact, over-rotation, can be seen here as the data points for the rotation are greater than 180 degrees. We must manually correct this artifact.
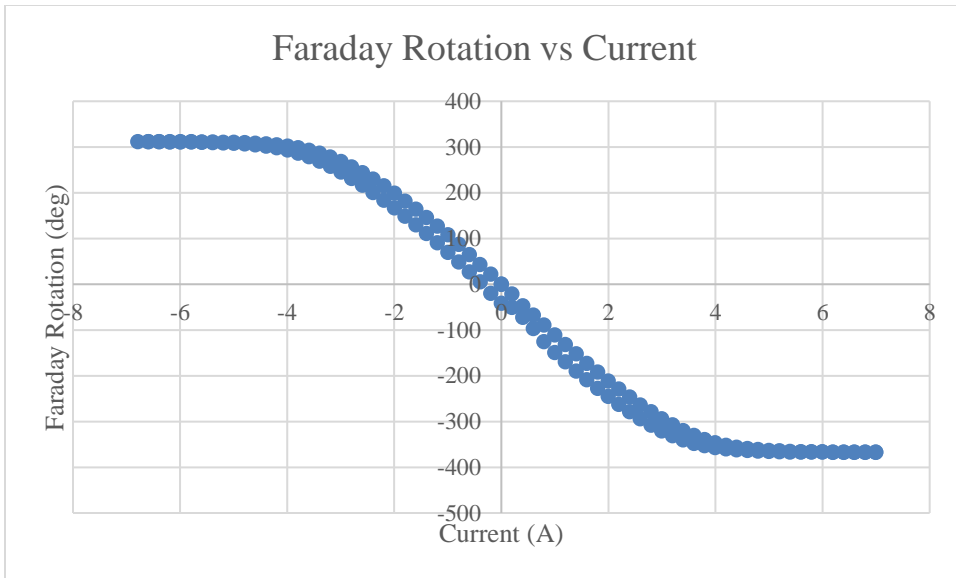
Fig. 7. *Mid-analysis data*

After correcting the data such that it shows the true value of the rotation, we obtain the above data. A fully-formed hysteresis loop can be seen with saturation points at either end where the current is maximized. This data now needs to be normalized to the thickness and we must obtain the total Faraday Rotation, the graph of which can be seen below.
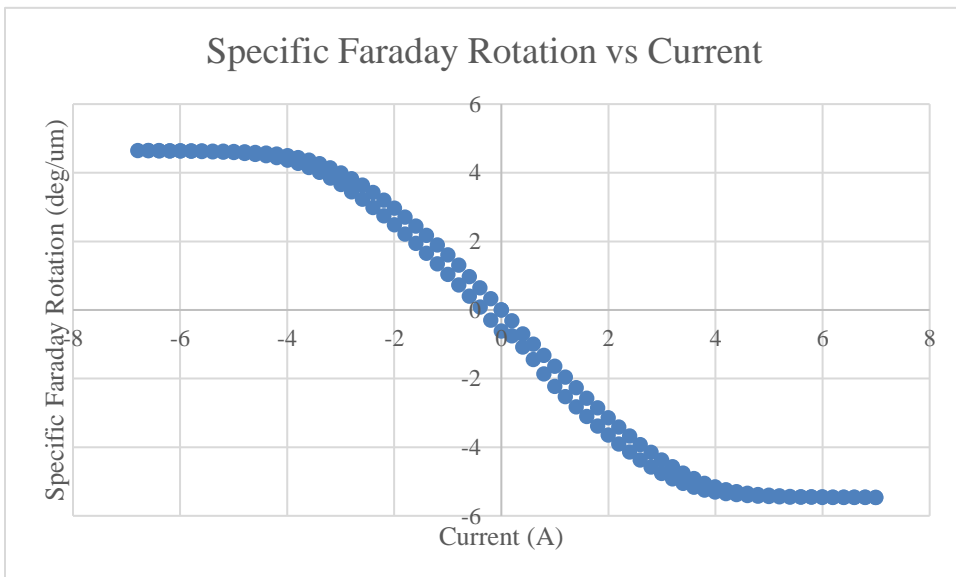

Fig. 8. *Fully-analyzed data*

Now that the data has been fully analyzed to reflect the reality of the data collected, we are able to obtain the specific Faraday rotation by taking the arithmetic mean of the "positive" and "negative" values of the Faraday rotation. We find the mean of the two points because the reference point for measuring the Faraday Rotation is arbitrary. We do not care about

the absolute value of the rotation but rather the relative rotation between the incident and emitted beam of light.

The data becomes harder to analyze as the thickness of the film is decreased. Noise and background from the substrate or other light sources in the room have a more prominent effect when the film is very thin and there are a few ways we attempt to remedy these negative effects. Primarily, we subtract out the contribution to the Faraday Rotation due to the GGG substrate of the material. We obtain the background contribution by performing a Faraday rotation measurement on a small piece of the sample that has had all of the film removed. The background data is seen below.
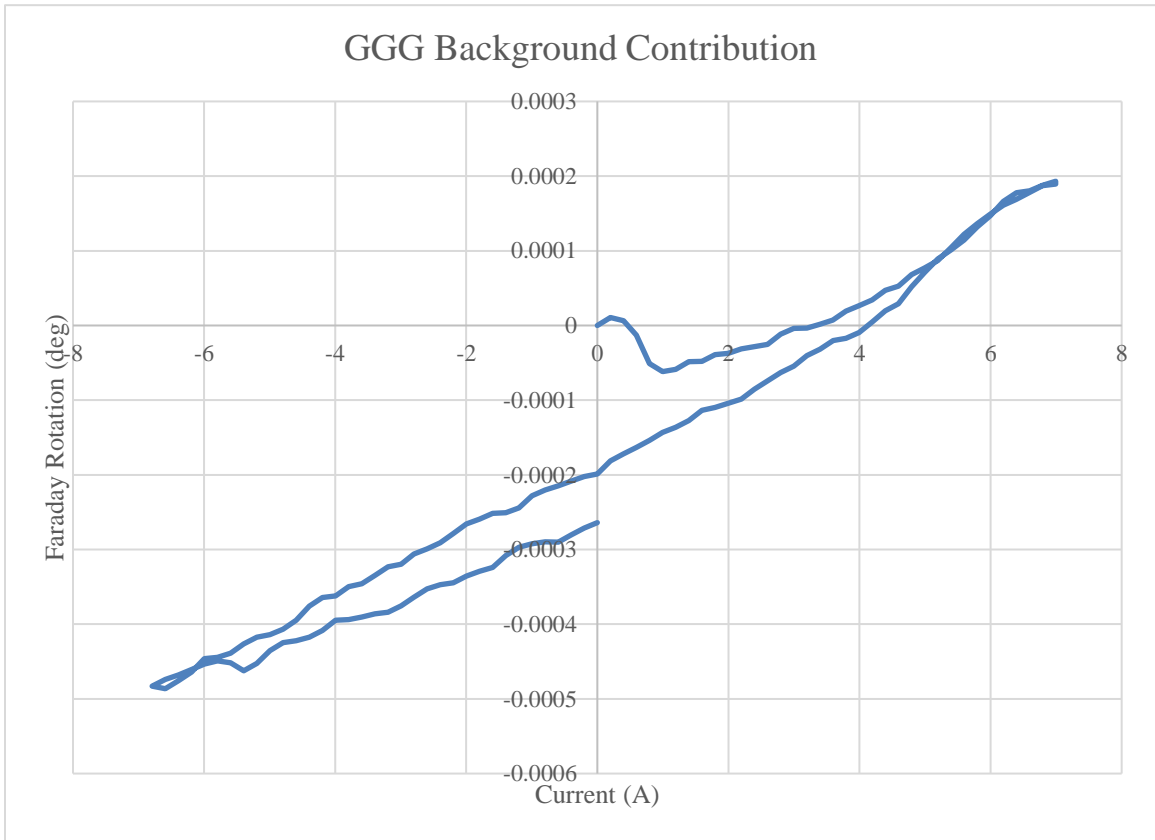

Fig. 9. *GGG background*

You may notice that the background is kept in terms of the total Faraday rotation opposed to the specific Faraday rotation. We subtract this background from the data before we normalize it to the thickness. A secondary method of reducing background and noise is by collecting the data in the dark. By shutting off any lighting that isn't the laser we drastically reduce the inherent noise that the sensor picks up.
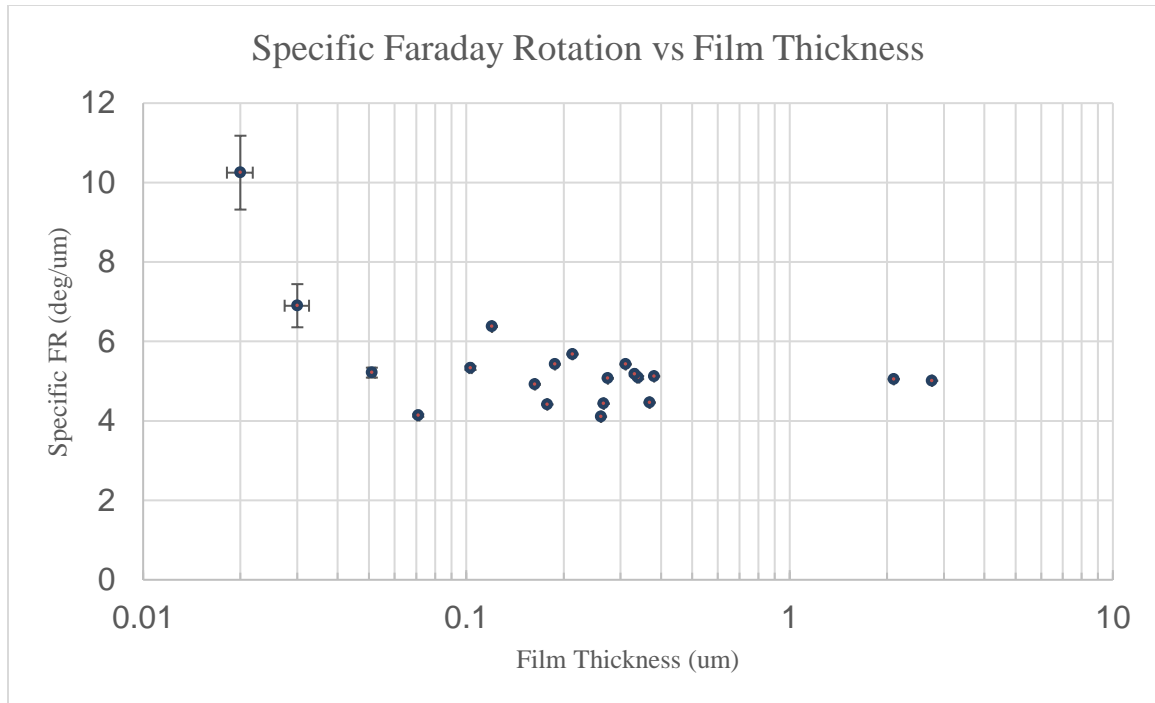
Figure 10, *Final Data Collected*

2.5 Error Analysis

There are three possible sources of error that result from the processes in this research. There is error that is the result of the method for etching, error from how the ellipsometer collects data and measures the thickness, and there is error is the consequence of how the Faraday rotation apparatus collects data. The wet-etching process has the inherent possibility of creating a radially uneven thickness of the film due to the angular rotation of the acid being stirred. While the width of the sample is small, it is possible for the angular velocity gradient to have an impact.

The errors for the thickness data points are a result of the diameter of the beam that the ellipsometer uses to collect data. The beam of the ellipsometer has a diameter of 1 mm which covers enough area that, given the possibility of non-uniform etching, has a gradient of film thicknesses. This source of error is small, with the uncertainty calculated by the ellipsometer typically around +/- <10 nm. This error is comparatively small at larger film thicknesses but becomes much more significant as the film thickness is decreased. This effect can be seen as the error bars are larger for the data points that are sub-100 nm in Fig. 7. The tertiary possible error source comes from the diameter of the laser used to measure the Faraday rotation for reasons similar to the ellipsometer error: the width of the beam allows for the possibility of transmitting through parts of the film with different thicknesses.

14

3 Discussion

3.1 General Discussion of Results

We have been able to replicate the significant enhancement of the specific Faraday rotation at ultra-thin thicknesses previously shown by A. Chakravarty. Our results also appear to confirm the presence of oscillations in the specific Faraday rotation in this iron garnet as the thickness approaches zero. Our colleagues in Russia recalculated their model using the new high-resolution data, the graph of which is shown below.
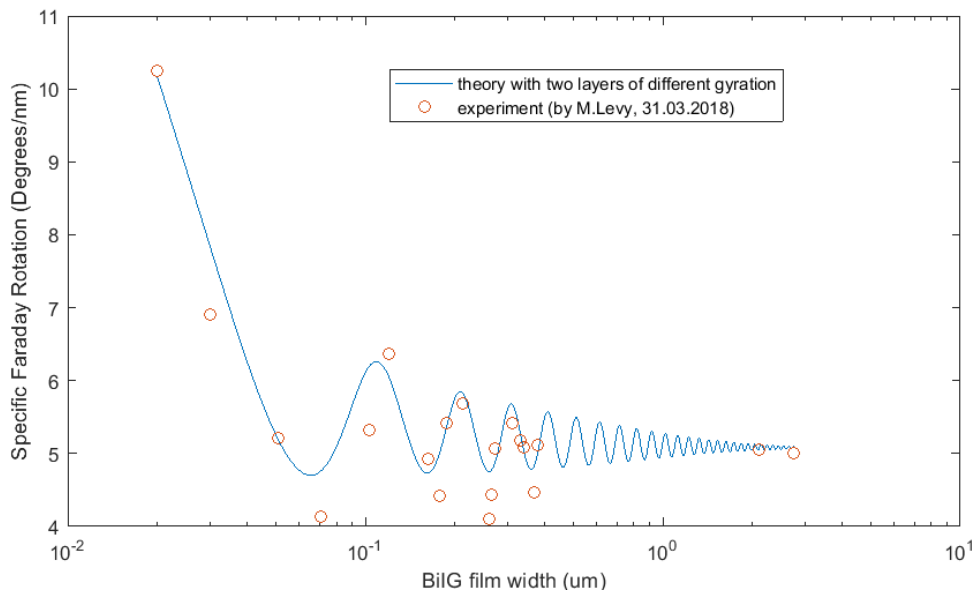

Fig. 11. *High-resolution Data (red) and model (blue)*

3.2 Phenomenological Discussion

While the model provides insight toward the general behavior of the Faraday rotation phenomenon at ultra-thin thicknesses, it can be seen that the model is unable to predict what the specific Faraday rotation will be at any given thickness. The shortcomings of the model are present in its inability to accurate predict the "wavelength" and "amplitude" of the oscillations. The model was derived on the basis that multiple reflections within the film itself cause changes in the specific Faraday rotation. When transmitted light reaches the film-to-air interface, some of the light is reflected back through the film and some of it is transmitted across the interface; this process occurs each time the light reaches a film-air interface. Backward propagating light is again reflected forward at the film-substrate

15

interface producing interference in the forward direction. This is the source of the oscillations in the Faraday rotation. Additionally, while the light is transmitting within the sample, the energy of the light is continuously absorbed by the material itself. The reflection process continues until the light is entirely absorbed.

We are certain that there are other effects in play that are causing this phenomenon. While the details of this phenomenon are still being investigated, we think that changes in electronic transitions and longer-lived electronic excitations are possible driving reasons for the enhancement of the Faraday rotation at ultra-thin thicknesses. Some of these quantum mechanical effects were already discussed in the original publication by Levy and Chakravarty reporting the Faraday rotation enhancement in ultra-thin films[2].

4 Reference List

[1]H. Nishihara, M. Haruna, and T. Suhara, *Optical Integrated Photonics* (Ohmhsa, Ltd., 1985).

[2]M. Levy, A. Chakravarty, H.-C. Huang, and R. M. Osgood Jr. Applied Physics Letters 107, 011104 (2015)

[3]O. V. Borovkova, H. Hashim, M. A. Kozhaev, S. A. Dagesyan, A. Chakravarty, M. Levy, and V. I. Belotelov. Applied Physics Letters 112, 063101 (2018)

[4]Jackson, John David (1998). Classical electrodynamics (3rd ed.). New York: Wiley.

[5] Vladimir Cherepanov; Igor Kolokolov & Victor L'Vov (1993). "The Saga of YIG: Spectra, Thermodynamics, Interaction and Relaxation of Magnons in a Complex Magnet". *Physics Reports*. pp. 84–144